

Analysis of Soil Erosion and Sediment Transport along a Rill Channel using a Sediment Transport Model

Azuma TAKAGI^{1*}, Seiji NAKAO² and Tatsumi TOMOSHO³

¹ Department of Hydraulic Engineering, National Institute for Rural Engineering (Tsukuba, Ibaraki 305–8609, Japan)

² National Agricultural Research Center for Western Region (Zentsuji, Kagawa 765–0053, Japan)

³ Department of Agricultural Environment Engineering, National Institute for Rural Engineering (Tsukuba, Ibaraki 305–8609, Japan)

Abstract

A mathematical model was developed to simulate soil erosion and sediment transport along rills in a field. For the model, a continuity equation for sediment with a term for the sediment transport capacity of rill flow was used. The Yang sediment transport equation was used to estimate this capacity. First, the equation of the model was solved under various intensities of rainfall events occurring during the observation, and the characteristics of the sediment load distribution along the rill in the field for study were clarified based on the results obtained. Second, net rill erosion at many positions along the rill was calculated using the solutions of the equations. Due to the good agreement between the calculated and observed values, the sediment transport model was found to be valid. Third, the effect of the sediment transport rate on the detachment rate along the rill was analyzed. The results showed that the effect was not appreciable in the case of moderate or higher rainfall intensity throughout the rill, while it became more pronounced when the distance along the rill increased under low intensity rainfall.

Discipline: Irrigation, drainage and reclamation

Additional key words: rill erosion, inter-rill erosion, sediment transport capacity

Introduction

Recently, studies based on sediment hydraulics and hydrology (Michael et al.⁸⁾, Borah¹⁾, and Nearing et al.¹²⁾ have contributed to the development of prediction equations and methods related to the rate of erosion, sediment discharge and volume of sediment transport. Croley and Foster²⁾, Hairsine and Rose⁵⁾ and Elliot and Lafren³⁾ have all conducted research on rill erosion. However, few studies have been carried out using the above prediction equations and methods in actual farmland, and in particular in reclaimed farmland.

Takagi et al.¹³⁾ have developed a prediction equation for the volume of erosion within rills by making a rill network, and they obtained good results by applying the equation of rill networks of higher orders developed on relatively steep and bare slopes. In that case, the development of rill networks divided the inter-rill basin into small segments. Therefore, it was observed that the lat-

eral inflow of sediments from the outer area into the rill was very small. Furthermore, for adapting the equation, it was assumed that the sediment transport capacity exceeded the sediment discharge at any point along the rill.

However, the lateral inflow of sediments from adjacent basins cannot be ignored for fields with a low rill density where slopes are gentle, and inter-rill basins associated with each rill are relatively large in the fields. In addition, the sediment transport capacity of such rills is lower than that for steeper rills. In some cases, the influence of sediment discharge of rills on the net erosion rate of rills must be considered.

In this study, the sediment transport model was applied to analyze the rill erosion and sediment transport in a rill within a parallel rill system formed in reclaimed farmland with a moderate slope under natural rainfall conditions. The study included the application of basic equations related to sediment transport, the use of the Yang sediment transport equation¹⁵⁾ as well as a recent

*Corresponding author: fax +81–298–38–7609, e-mail takagia@nkk.affrc.go.jp

Received 29 September 2000, accepted 26 February 2001.

investigation conducted by Moore and Burch⁹⁾. The sediment transport capacity and sediment inflow into rills were calculated under natural rainfall conditions. The characteristics of the sediment discharge within a rill and the volume of the erosion and sediment discharge of a rill were analyzed, and finally the effectiveness of the model was evaluated under natural rainfall conditions. In addition, in this study, the influence of sediment discharge on the erosion rate in a rill was analyzed.

Numerical model of sediment movement along a rill

1) Equations for sediment movement along a rill

The continuity equation of sediment for a rill is:

$$\frac{\partial}{\partial t}(AC) + \frac{\partial}{\partial x}(QC) = D_r + q_s \quad (1)$$

where C = sediment concentration (kg/m³); A = cross-sectional area of rill flow (m²); Q = rill flow discharge (m³/s); D_r = rill erosion rate (kg/m/s); q_s = lateral sediment inflow from inter-rill areas to rill flow (kg/m/s); x = downslope distance (m); and t = time (s).

The following equation was obtained by solving the balance equation presented by Foster and Meyer⁴⁾, which defines the interaction between the sediment discharge and sediment transport capacity of flow, for D_r .

$$D_r = \left(1 - \frac{G}{T_c}\right)D_{rc} = \left(1 - \frac{QC}{T_c}\right)D_{rc} \quad (2)$$

where G = sediment discharge (kg/s); therefore, $G = QC$, D_{rc} = erosion capacity of rill flow (kg/m/s); and T_c = sediment transport capacity of rill flow (kg/s).

By substituting Equation (2) into Equation (1), we obtain:

$$\frac{\partial}{\partial t}(AC) + \frac{\partial}{\partial x}(QC) = \left(1 - \frac{QC}{T_c}\right)D_{rc} + q_s \quad (3)$$

In the case of steady flow using Equation (3), we obtain:

$$\frac{dG}{dx} = \left(1 - \frac{G}{T_c}\right)D_{rc} + q_s \quad (4)$$

The erosion capacity of the rill flow can be estimated based on the results of the previous study¹³⁾ and expressed as:

$$D_{rc} = aQ^bS^c \quad (5)$$

where Q = rill flow discharge (m³/s); S = slope of a rill; "a" = coefficient of configuration of cross section and erodibility of soil; and "b" and "c" are exponents.

2) Surface runoff model

In this analysis, as will be discussed later, every runoff duration time will be divided into smaller intervals in order to approximate Equation (3) by the steady-state sediment continuity equation (Equation (4)). In this case, the discharge within rills, as indicated in the previous study¹³⁾, can be approximately evaluated by using the following runoff model:

$$Q = \frac{1}{3.6} \times 10^{-6} A_*(x) r_{e,i} \quad (6)$$

where $A_*(x)$ = catchment area (m²) of x m at the downstream point of a rill; $r_{e,i}$ = average intensity of effective rainfall for a time interval [t_i, t_{i+1}] in (mm/h).

When a non-steady condition in rainfall-runoff phenomena tends to prevail, to predict accurately the distribution of the erosion rate and sediment discharge as a function of the distance x along the rill channel and time t , a distribution flow routing model such as the kinematic wave runoff model should be used.

3) Sediment transport capacity of rill flow

(1) Yang sediment transport equation: Yang¹⁵⁾ adopted the concept of unit stream power, and thus developed the following estimation equation of sediment transport,

$$\log_{10} C_t - \gamma = \beta \log_{10} \left\{ (VS_f - V_{cr}S_f) / \omega \right\} \quad (7)$$

where C_t = sediment concentration (ppm by weight); V = flow velocity (m/s); V_{cr} = critical flow velocity (m/s) in which sediment can not be transported below the critical value; and S_f = energy gradient. When pseudo-steady flow is assumed, then, VS_f and $V_{cr}S_f$ are, respectively, equal to VS and $V_{cr}S$, where S is a channel gradient. ω = sediment terminal fall velocity in water (m/s). β and γ are expressed in Equations (8) and (9), respectively:

$$\beta = 1.799 - 0.409 \log_{10}(\omega d / \nu) - 0.314 \log_{10}(U_* / \omega) \quad (8)$$

$$\gamma = 5.435 - 0.286 \log_{10}(\omega d / \nu) - 0.457 \log_{10}(U_* / \omega) \quad (9)$$

where U_* = shear velocity (m/s), thus $U_* = (gRS_f)^{0.5}$; R = hydraulic radius (m); g = acceleration due to gravity (m/s²); d = medium diameter (m) of soil particles; and ν = kinematic viscosity (m²/s) of flow.

Thus, according to Moore and Burch⁹⁾, by adopting Yang Equation (7) as an estimation equation for sediment transport capacity, the sediment transport capacity T_c (kg/s) of the rill flow in Equation (4) can be derived by substituting C_t in Equation (7) into the following equation:

$$T_c = C_t \cdot Q \times 10^{-3} \quad (10)$$

where Q = rill flow discharge (m^3/s).

(2) Calculations of V_S and $V_{cr}S$: Based on Moore and Burch⁹⁾ studies, V_S in the rill of Equation (7) can be determined by the following equation:

$$V_S = Q^{0.25} S^{1.375} W / n^{0.75} \quad (11)$$

where n = Manning roughness coefficient; W = rill shape factor, assuming that the following regime rule can be used:

$$R = W^2 A^{1/2} \quad (12)$$

where R = hydraulic radius (m); and A = flow area of rill (m^2). Assuming that the cross section of the rill flow is rectangular, according to Moore and Burch⁹⁾, W can be expressed in the following equation:

$$W = \{a_*^{0.5} / (a_* + 2)\}^{0.5} \quad (13)$$

where a_* = (width of rill)/(flow depth of rill). For $a_* = 2$, the maximum value of W is 0.595, while for $a_* = 1 \sim 5$, the value W does not vary appreciably. W ranges from $W = 0.565$ ($a_* = 5$) to $W = 0.595$ ($a_* = 2$). In this study, the flow area was assumed to be rectangular in shape and was assigned the average value of $a_* = 3$. Then, using Equation (13), $W = 0.589$ was obtained.

Based on Yang Equation¹⁵⁾, the value of V_{cr} can be calculated using the following equations:

$$V_{cr}/\omega = 2.5 / (\log_{10} R_e^* - 0.06) + 0.6 \quad (0 < R_e^* < 70) \quad (14a)$$

$$= 2.05 \quad (R_e^* \geq 70) \quad (14b)$$

where $R_e^* = U_* d / \nu$. Thus, $V_{cr}S$ can be determined by using Equation (14a) or (14b).

(3) Calculation of U_* : In the case of a steady flow, by using the Manning Equation, Equation (12) and the continuity equation of flow, $Q = AV$, the following estimation of U_* can be made:

$$U_* = g^{1/2} n^{3/16} W^{3/4} Q^{3/16} S^{13/32} \quad (15)$$

4) Sediment inflow from inter-rill basin

(1) Estimation equation for sediment inflow: Assuming that the catchment area for the head of a given rill (hereafter referred to as "source catchment") can be represented approximately by a rectangle, by assigning the

unit, kg/s and using Komura erosion equation⁶⁾, the sediment inflow $G_i(0)$ from a source catchment to a rill channel is:

$$G_i(0) = \frac{1}{3.6} \times 10^{-3} K B r_e^{15/8} L^{11/8} S_o^{3/2} \quad (16)$$

where r_e = intensity of effective rainfall (mm/h); L = source catchment length (m); S_o = average slope gradient of a source catchment; B = average width of a source catchment (m); and K = coefficient provided by the equation below.

$$K = 8.73 \times 10^{-7} C_A C_E W_s / d_m \quad (17)$$

where C_A = rate of bare surface area; C_E = erodibility coefficient; W_s = unit weight of the soil (kg/m^3); and d_m = average grain size (mm). According to Komura⁷⁾, C_E can be expressed in the following equations:

$$C_E = 0.17 C_M (1 + 3.67 R_d) / (CR/DR) \quad (CR/DR > 0.0425) \quad (18a)$$

$$= 4 C_M (1 + 3.67 R_d) \quad (CR/DR \leq 0.0425) \quad (18b)$$

where C_M = compaction factor of soil, R_d = rill density, CR = clay ratio, $CR = \text{Clay}(\%) / [\text{Sand}(\%) + \text{Silt}(\%)]$, and DR = dispersion ratio of Middleton.

Furthermore, by using Komura erosion model, an equation for the estimation of the lateral sediment inflow per unit length of rill ($\text{kg}/\text{m}/\text{s}$) can be obtained as:

$$q_s = \frac{1}{3.6} \times 10^{-3} K r_e^{15/8} l^{11/8} S_l^{3/2} \quad (19)$$

where K and r_e are the same as in Equation (16); l = flow length (m) of the lateral inflow and S_l = slope in the flow direction.

Field plot for study

In order to apply the sediment transport model described in the previous chapter, a field plot for study was constructed in a reclaimed farmland located within the Ohashi District in the hilly area of Fukuyama City suburbs, Hiroshima Prefecture. The surface soils in the farmland were derived from decomposed granitic rocks.

For this investigation, the duration of the period of study (hereafter referred to as "study period") extended from June 20 to July 18, 1989. The field plot was nearly bare during the study period. In the early part of the study (June 20, 21) and at the end of the study period (July 18), the following investigations were conducted:

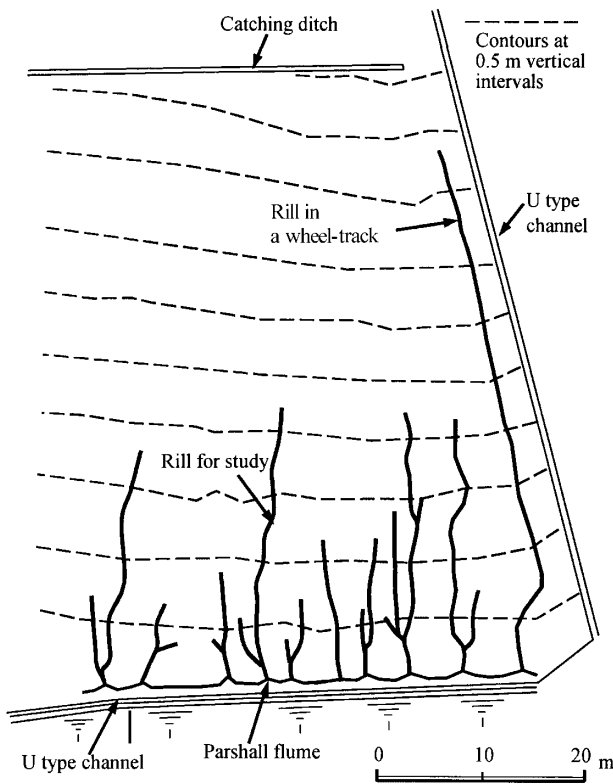


Fig. 1. Map of rill systems in the field for study

(1) a detailed topographic survey of the field plot; (2) survey of the rill system configuration that developed within the field plot (only on June 20); (3) survey of the cross sections of the rills; and (4) survey of the longitudinal sections of the rills. During the survey of the cross and longitudinal sections of the rills, one of the main rills that developed in the field plot was selected (Fig. 1). The total length of the rill for study (hereafter referred to as “study rill”) was 25.4 m. The locations of the cross section survey points were determined as the distance from the rill head to each survey point, and are shown along the x-axis in Fig. 4. The measurements of the rill configuration at the locations were recorded at around 1 cm

Table 1. Properties of soil collected in the center of the field plot for study

Particle size range (0–10 cm layer)	mm	%
>0.2		12
0.2–0.074		69
0.074–0.005		17
<0.005		2
Dispersion ratio (0–10 cm layer)		16%
Specific gravity (0–10 cm layer)		2.660
Bulk density	(0–10 cm layer)	1.53 Mg/m ³
	(10–20 cm layer)	1.55 Mg/m ³

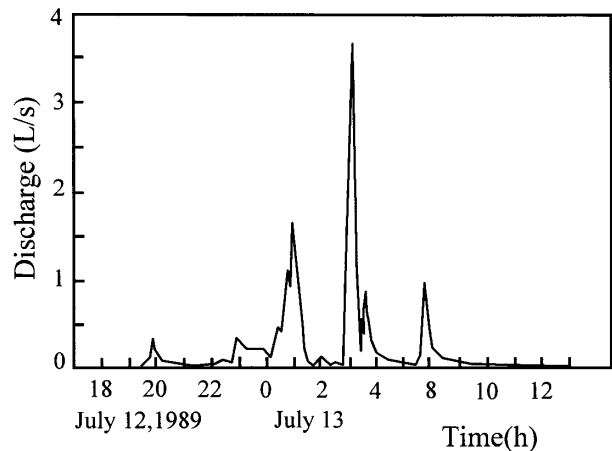


Fig. 2. Typical hydrograph of the outlet in the catchment of the rill for study

along the base lines. While constructing cross and longitudinal sections, 4 soil samples from about 15 cm below the ground surface at several locations along the study rill were collected to determine the dry density and other physical properties. On June 21, 1989, a Parshall flume was placed along the lower end of the study rill (Fig. 1), and discharge measurements were initiated. Also, a rain

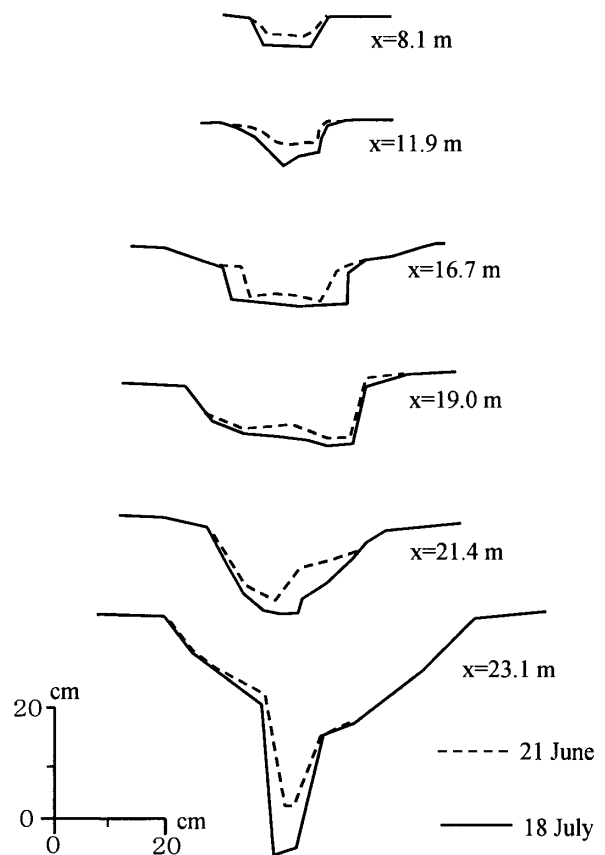


Fig. 3. Typical rill cross sections along the rill for study

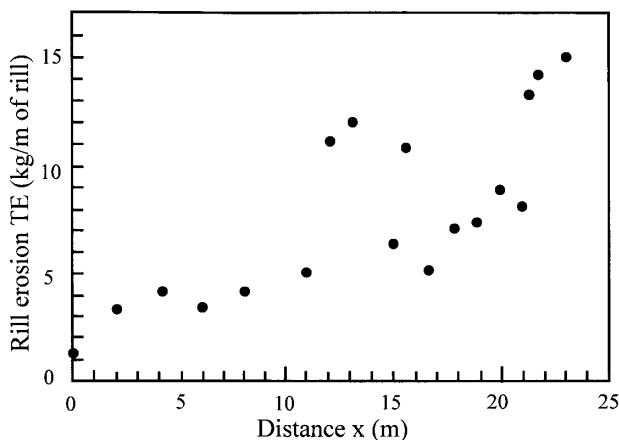


Fig. 4. Rill erosion observed along the rill for study
 x: Distance from the upstream edge of the rill for study.

gauge was established near the site to measure the rainfall intensity.

The physical properties of the surface soils collected from the middle section of the study rill are shown in Table 1.

Based on a detailed survey at the early stage of the study of the field plot, the configuration of the rill system is shown in Fig. 1. The total length of the slope for the field plot for study between the upper diversion ditch and the lower U-type channel was 57 m. The inclination of the field plot was fairly uniform with an average value of 0.08 (or 4.59°). As shown in Fig. 1, a series of rills developed in parallel. A few small-scale rills about 50 cm long with a 2 to 3 cm depth developed along the study rill over the study period. Also, there was only a very minor extension of the main trunk of the rills.

Eight rainfall events led to runoff at the lower end of the rills during the study period. Based on the discharge data, runoff hydrographs for each of the 8 rainfall events were constructed. A typical runoff hydrograph is shown in Fig. 2.

Some of the representative cross sections of the study rill constructed on June 21 and July 18, 1998 are shown in Fig. 3. Based on the changes in the configuration of the cross sections observed between June 21 and July 18, it was assumed that the erosion process of the rill was primarily limited to marked erosion in the wetted perimeter zone by the flow within rills. However, based on the changes in the configuration of the cross sections at 3 locations along the mid-stream portion (locations: 11.9, 13.0, and 15.7 m), active small-scale failures along the rill side walls were detected.

First, the changes in the cross-sectional areas between June 21 and July 18 were analyzed at each station along the rill. Then the volume of rill erosion of the

unit rill length for each station selected during the study period was calculated based on the changes in the cross-sectional areas and data on dry density, γ_d of surface soil along the rill. The observed rill erosion along the study rill is shown in Fig. 4.

Solution of the differential equation of sediments

In this analysis, for each time interval, $t_i \leq t \leq t_{i+1}$ ($i=1, 2, \dots, n$) in a runoff period, a steady state of flow in the rill was assumed. Therefore, the differential equation of sediments, Equation (4), was used for each time interval. Furthermore, it was found that since the intensity of effective rainfall was uniform for each time interval, the influence of the time of flood concentration could be ignored.

Sediment discharge at any point along a rill for each $r_{e,i}$ value can be determined by solving Equation (4) for an average intensity of effective rainfall $r_{e,i}$ for each time interval $[t_i, t_{i+1}]$. Equation (4) was numerically solved in relation to $r_{e,i}$ by using the Runge-Kutta method.

Furthermore, in order to solve Equation (4), the following assumptions were made: 1) During the study period, there was no time variation in the catchment area $A^*(x)$ (m^2) at any point $x(m)$ along a rill; 2) The majority of the runoff that occurred within the field plot (Fig. 1) was assumed to be drained through the rills developed in the field; 3) The time variation of slope $S(x)$ of the rill during the study period could be ignored; 4) Flow length of influent to rill from the inter-rill basin was temporally and spatially constant. The results of this erosion investigation supported the assumptions 1) and 3).

1) Catchment area $A^*(x)$ and channel gradient $S(x)$ of rill

Based on the assumptions 1) and 2) and the assumption that the inter-rill areas and catchments where outlets are rill heads were rectangular, the catchment area of the rill at point x was determined. The average width of the inter-rill was determined by the interval between the 2 central lines of the areas between the study rill and adjacent left or right bank rill, and the average width of the catchment was determined by the lines extending to the uppermost boundary of the field plot. Moreover the length of the catchment was determined by the distance between the uppermost boundary and the rill head for study. Consequently, the catchment area $A^*(x)$ was expressed as:

$$A^*(x) = 4.36x + 122.0. \quad (20)$$

Based on assumption 3) above and the results of the

longitudinal section survey of the study rill at the beginning of the field investigation, the gradient $S(x)$ of the rill channel was determined. The values of $S(x)$ were 0.092 for the upstream section, 0.095 for the mid-stream section, above 0.120 for the lower stream section, and reached a maximum of 0.165 for the lowest stream section.

2) Division of runoff time and intensity of effective rainfall

Every runoff duration time was subdivided into smaller intervals $[t_i, t_{i+1}]$ to 300 s. Here, the runoff duration time refers to the time from the initiation of runoff to the time when the discharge at the end of the rill for study was less than 0.051 (L/s).

For each runoff event during the study, the average rainfall intensity $r_{e,i}$ for each time interval $[t_i, t_{i+1}]$ was determined. Actually, based on the runoff hydrograph of the lower end of the rill, as indicated in the previous chapter, the average discharge of the divided time intervals was determined. Then using Equation (21), $r_{e,i}$ (mm/h) was calculated:

$$r_{e,i} = 3.6 \times 10^6 (Q/A_o) \quad (21)$$

where Q = average discharge (m^3/s) of the divided time intervals at the lower end of the rill; and A_o = total catchment area (m^2) at the lower end of the rill.

3) Initial conditions

As the channel length was subdivided into $0 \leq x \leq 13.5(\text{m})$, $13.5 \leq x \leq 20.5(\text{m})$, $20.5 \leq x \leq 22.5(\text{m})$, and $22.5(\text{m}) \leq x$, the channel gradient was assumed to be uniform within each channel segment. Therefore, Equation (4) was solved according to each subdivision. Thus, it was necessary to provide initial conditions $G(0)$, $G(13.5)$, $G(20.5)$, and $G(22.5)$ for each corresponding channel segment.

$G(0)$ is equal to the sediment inflow to the rill head in a unit time and can be determined by the method described in section 6) of this Chapter. The initial conditions other than $G(0)$ can be determined by numerical solutions within the corresponding channel sections.

4) Calculation method for erosion capacity D_{rc} of rill flow

Equation (5) was used to calculate the erosion capacity D_{rc} ($\text{kg}/\text{m}/\text{s}$). Furthermore, runoff model Equation (6) and Equation (20) were used to calculate the discharge within the rill.

In this analysis, based on the previous study¹³⁾, $b = 1.0$ and $c = 1.3$ were used for b and c in Equation (5). Due to the paucity of the studies or data to determine the value of coefficient "a" with a high degree of accuracy, "a" was

determined by using the observed data of sediment yield from rill erosion. For the rill gradient S , as discussed in section 3), the rill channel was divided into 4 segments and it was assumed that the gradient was uniform within each segment.

5) Evaluation method for sediment transport capacity of rill

Yang Equations (7) and (10) were used to evaluate the sediment transport capacity of a rill. Equations (8) to (15), (except for Equation (10)) were used to calculate variables and coefficients for Equation (7). That is for each runoff event during the study period, the distribution of T_c along the major part of the study rill reach was determined at every 1 m interval for every case where the average intensity of effective rainfall $r_{e,i}$ was obtained for 300 s intervals, as discussed in section 2) of this chapter, while for flow intervals of 20 ~ 21 m and 22 ~ 24 m from the rill head, 0.5 m intervals were used. For the calculations, based on the report of Mosley and others^{10,11)}, the roughness coefficient, $n = 0.03$ was adopted. The settling rate ω of soil particles was determined by Rubey fall velocity equation using the results of grain size distribution analysis and density tests. From this analysis, it was determined that for all the $r_{e,i}$ values for each channel segment of rill which is assumed to have a uniform channel gradient, T_c increased linearly as the distance from the rill head $x(\text{m})$ increased and it could be accurately approximated as a linear function. Then, the regression lines of T_c in relation to each $r_{e,i}$ value and channel segments were obtained by the method of least squares. In order to solve Equation (4), these regression equations were used.

6) Calculation method for sediment inflow to rill

The validity of Komura equation was confirmed based on the data of rainfall, surface flow rate and sediment discharge, which were collected for each rainfall event in an experimental plot at the National Agricultural Research Center for Western Region located in Hiroshima Prefecture¹⁴⁾.

(1) Determination of the flow length L , l and flow gradient S , S_i : In order to calculate $G(0)$ for each $r_{e,i}$ value, by using Equation (16), the slope length of the basin which has the rill head as its outlet, $L(\text{m})$ was determined to correspond to the total flow length from the uppermost watershed divide of the rill catchment to the rill head. The gradient of the catch basin, based on the survey results, was $S = 0.08$.

In order to calculate the lateral sediment inflow for a unit time and unit channel length of rill by using Equation (19), the flow length $l(\text{m})$ of the influent was derived in the following manner. From the directions of small tribu-

tary rills into the main rill, the directions of the influent were determined, and l , the distance between the inflow point and the drainage divide of the main rill, was measured. The gradient S_i , was assumed to be the gradient of the ground surface of the inflow direction (inter-rill zone).

(2) Determination of parameter K : The K -value of the inter-rill zone in the field plot for the rill erosion study can be determined from Equations (17) and (18a) or (18b). From Equation (17), $K = 4.93 \times 10^{-3}$ was derived. This K -value was used to calculate q_s in Equation (19) and to calculate $G(0)$ in Equation (16).

Numerical analysis of volume of erosion in rill and sediment load

1) Sediment discharge along rill and sediment load from rill

(1) Sediment load from rill and determination of parameter α : The total sediment load TTG (kg) from the channel reach from the rill head to a downstream point, x (m) during the study period was estimated by the equation:

$$TTG = \sum_{j=1}^m \sum_{i=1}^{n(j)} G_{i,j}(x) \Delta t_{i,j} \quad (22)$$

Where m = number of rainfall-runoff events which occurred during the study period; $G_i(x)$ = average sediment discharge (kg/s) at point x (m) for time interval $[t_i, t_{i+1}]$ during an average intensity of effective rainfall $r_{e,i}$ (mm/h); and $\Delta t_i = t_{i+1} - t_i$ (s). $G_{i,j}(x)$ and $\Delta t_{i,j}$ indicate the j th occurrence of the rainfall-runoff event; and $n(j)$ indicates the number of events n as a function of j .

Of which, the total sediment load (kg) attributed to rill erosion is:

$$TTG_r = \sum_{j=1}^m \sum_{i=1}^{n(j)} \{G_{i,j}(x) - (G(0) + q_{s,i,j} \times x)\} \Delta t_{i,j} \quad (23)$$

By using the observed value of the total sediment yield from erosion in the channel interval $0 \leq x \leq 23.1$ (cm) and Equation (23), the parameter “ a ” of the erosion model (5) can be determined. As a result, $a = 10.12$.

The measurements of the sediment load for the calculation were derived in the following manner. The total volume of erosion within the channel segment, from the rill head to point 23.1 m, was determined from the measurements of the volume of rill erosion and distances of each measurement point as described in the previous chapter. The amount of erosion from 3 locations in the middle reach of the rill (described in the previous chapter) was not directly used as raw data. For these locations, data interpolated from the adjacent area were utilized. Based on this calculation method, the total vol-

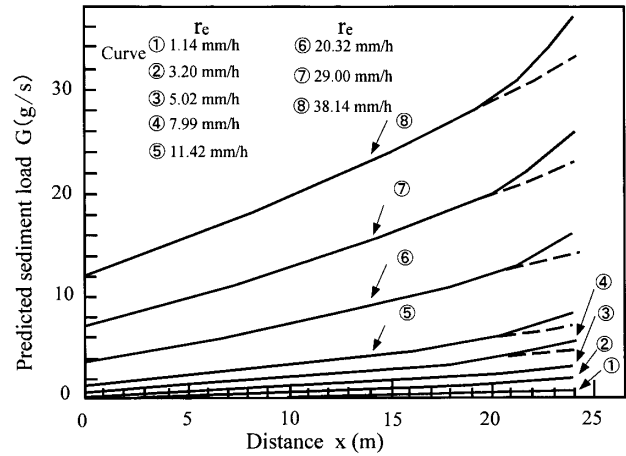


Fig. 5. Predicted sediment load along the rill for study

The dashed lines represent the simulated curves when the slope of the rill is constant (=0.092). x : Distance from the upstream edge of the rill

ume of erosion of the channel segment $0 \leq x \leq 23.1$ (m) during the study period was 134.44 (kg). Consequently the observed value of the total volume of rill erosion 134.44 (kg) was used to determine the value of “ a ”.

By using $a = 10.12$, and based on Equation (22), the total sediment runoff during the study period from the channel segment, rill head to near the end of the field, when $x = 23.1$ (m), and $m = 8$, was estimated at 170.44 (kg). Based on Equation (23), and when $x = 23.1$ (m), and $m = 8$, the calculation of the total sediment load, TTG_r , due to rill erosion, was estimated at 134.51 (kg).

(2) Distribution of the sediment discharge along the rill: Fig. 5 shows representative distribution curves of the sediment discharge $G = G(x)$ (where x is the rill flow distance (m)) of the rill derived by solving the differential Equation (4). In this case, the above value of “ a ” was used. The graph presents 3 cases: low intensity of effective rainfall ($r_{e,i} = 1.142, 3.197$ (mm/h)); medium intensity ($r_{e,i} = 5.024, 7.992, 11.418$ (mm/h)) and high intensity ($r_{e,i} = 20.324, 29.000, 38.135$ (mm/h)). The $r_{e,i}$ value of 38.135 (mm/h) corresponded to the highest intensity among the $r_{e,i}$ values determined by the calculations. This value corresponded to the intensity of effective rainfall for a time interval including the start of the peak runoff of actual rainfall of the largest rainfall-runoff event during the study period. As shown in Fig. 5, dG/dx increased as $r_{e,i}$ increased. Moreover, $G = G(x)$ almost linearly increased with x , along the downstream direction. At lower reaches, G increased rapidly when the runoff increased in the rill slope. The dashed lines indicate the expected distribution curves of the sediment discharge $G = G(x)$ by assuming that the middle and lower reaches of the rill gradients were the same as those of the

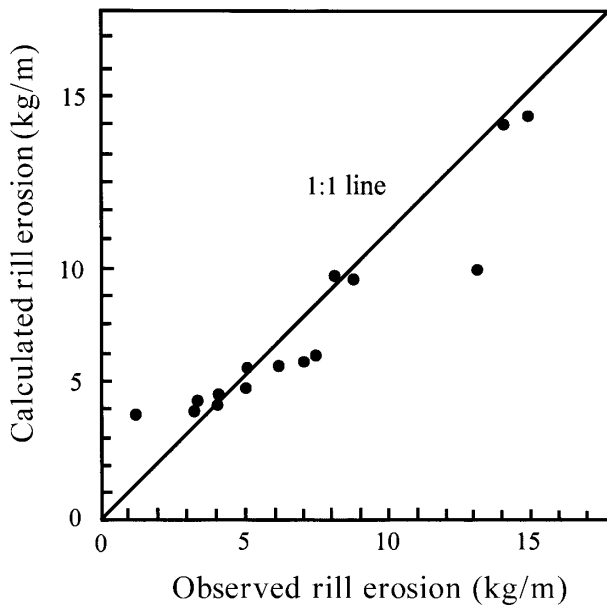


Fig. 6. Calculated versus observed values of rill erosion at the positions along the rill for study

upper reaches (0.092) for each $r_{e,i}$ value. By comparing the distribution curves of the sediment discharge of the actual rill gradient with the distribution curves, assuming that the gradients of the middle and lower reaches were the same as those of the upper reaches, the sediment discharge tended to drastically increase at the lower reaches and was strongly influenced by the fact that the rill gradient increased in the downstream direction.

2) Volume of erosion in each flow segment of rill

The total volume of erosion at each flow point x during the study period is estimated by:

$$TTD = 1.012 \times 10 \sum_{j=1}^m \sum_{i=1}^{n(j)} \{1 - G_{i,j}(x)/T_{c,i,j}(x)\} \cdot Q_{i,j}(x) \cdot \{S(x)\}^{1.3} \cdot \Delta t_{i,j} \quad (24)$$

where TTD = total volume of rill erosion (kg/m) of a unit channel length during the study period; $T_{c,i,j}(x)$ and $Q_{i,j}$ are, respectively, the transport capacity (kg/s) of the rill flow and the rill flow discharge (m^3/s) in $\Delta t_{i,j}$ during the rainfall event j th; and $G_{i,j}(x)$, $\Delta t_{i,j}$ and subscript j are, respectively, the same as in Equation (22). Then, using the distribution curves of the sediment discharge $G = G(x)$ for each $r_{e,i}$ value determined in the previous section, the volume of rill erosion during the study period for each flow point in the rill (refer to Fig. 4) was calculated. The results of the calculation are shown in Fig. 6. However, locations where excess side wall erosion occurred in the middle of the channel were excluded from this calculation.

As shown in Fig. 6, except for 2 locations, the calculated and observed values of rill erosion were in good agreement. The above results indicate the suitability of the sediment model equations.

3) Influence of sediment discharge on rill erosion rate and volume of erosion

In order to examine the degree of influence of the sediment discharge G on the true erosion rate D_r , we defined the term, $1 - G/T_c$ in Equation (2) as the index of the degree of influence.

By substituting the term for α , we obtain:

$$\alpha = 1 - G/T_c \quad (25)$$

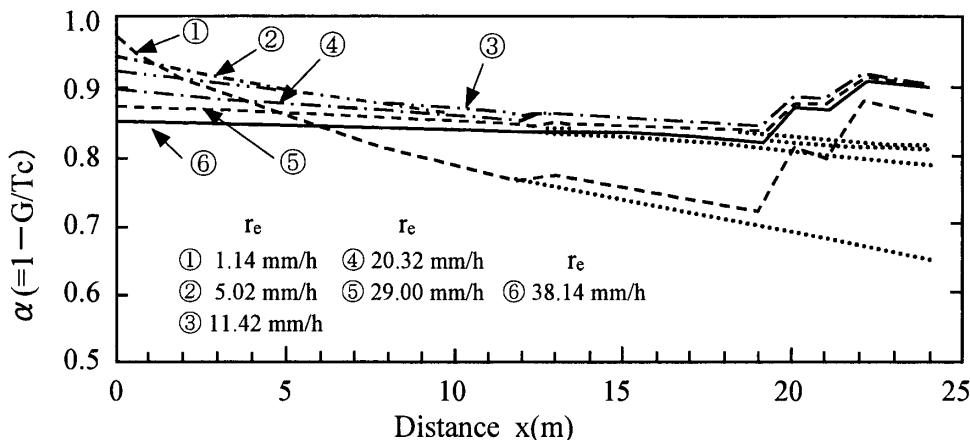


Fig. 7. Changes in α values along the rill for study

The dotted lines represent the simulated curves when the slope of the rill is constant (=0.092).
 x : Distance from the upstream edge of the rill.

When the transport capacity of the flow is much higher than the sediment discharge G , α is nearly equal to 1, indicating that G hardly affected the actual erosion rate D_r .

In order to identify the degree of influence, using the results of calculations for $G = G(x)$ solved in the previous section, and using Equation (25), the value of α at each flow location for each intensity of effective rainfall $r_{e,i}$ can be calculated. Fig. 7 shows the representative distribution curves of the value of α along the flow direction of the rill for each $r_{e,i}$ value and are denoted by a solid line. Like in Fig. 5, the graphs depict 3 representative cases. These cases are identical with those set up for analyzing the sediment discharge distribution in section 1) of this chapter. Assuming that the gradients of the middle and lower reaches are the same as those in the upper reaches, the distribution curves of α are denoted by dotted lines.

As shown in the graph, for most of the $r_{e,i}$ values, the value of α gradually decreased along the flow, i.e. the x -direction. The value was the smallest at the upper end of the lower reaches and then increased toward the rill outlet. For higher than average values of $r_{e,i}$, the variation of α along the x -direction, except for the channel segment $x = 19 \sim 22$ m, was very small. Especially, when the intensity of effective rainfall exceeded the average value for which the volume of erosion and sediment load were strongly affected, the maximum value of α ranged between 0.92 and 0.95 while the minimum value was about 0.83.

Thus, it was demonstrated that even in the field plot for study which has a low rill density with relatively gentle slopes without significant rill development, for a higher than moderate rainfall intensity and higher sediment transport capacity of rill flow which markedly exceeds the actual sediment discharge in the rill, the true erosion rate and volume of erosion were not appreciably influenced by the sediment discharge.

Furthermore, based on the distribution curves of α , assuming that the gradient value of the upper reaches of 0.092 was similar to that of the middle and lower reaches, the value of α decreased to 0.65 for a weak rainfall intensity. For a moderate rainfall intensity, the value of α was about 0.8, and was close to 0.8 for a strong rainfall intensity along the downstream reaches. Based on the results of the simulation for α , if the gradient of the lower reach is the same as the gradient of the upper and middle reaches, it was assumed that the erosion rate and volume of erosion may be influenced by the sediment discharge. These results also suggest that in long main rill channels whose lower reaches have gentle slopes, the influence of the sediment discharge on the net erosion rate, volume of

erosion and the sediment yield cannot be ignored.

Conclusion

The differential equation of the model for predicting rill erosion and sediment transport was solved by numerical calculations for various intensities of effective rainfall that occurred during the study period. Based on these numerical solutions, the volume of erosion at each location along a rill was determined. For most of the locations, the calculated values and observed values showed a good agreement, indicating that the sediment transport model proposed in this paper is valid. Using this model and by providing an appropriate parameter “ a ”, the volume of erosion and sediment load of any location along the rill channel could be estimated with a high degree of accuracy. In addition, various estimations regarding the distribution characteristics of the sediment discharge along the flow direction of a rill were analyzed by numerical equations. Furthermore, based on the results of these calculations and by examining the influence of the sediment discharge on the erosion rate, it was found that the influence was not appreciable when the average rainfall intensity was more than average, which contributes significantly to the volume of erosion and sediment load. The variation in the degree of influence on the lower reaches was also negligible, suggesting the validity of the application of Equation (5) for a model to estimate the rill erosion rate when a rainstorm occurs.

References

- 1) Borah, D. K. (1989): Sediment discharge model for small watersheds. *Trans. ASAE*, **32**(3), 874–880.
- 2) Croley II, T. E. & Foster, G. R. (1984): Unsteady sedimentation in nonuniform rills. *J. Hydrol.*, **70**, 101–122.
- 3) Elliot, W. J. & Lafren, J. M. (1993): A process-based rill erosion model. *Trans. ASAE*, **36**(1), 65–72.
- 4) Foster, G. R. & Meyer, L. D. (1972): A closed-form soil erosion equation for upland areas. *In Sedimentation, Symposium to Honor Professor H. A. Einstein*. ed. Shen, H. W., Fort Collins, Colo., 12.1–12.19.
- 5) Hairsine, P. B. & Rose, C. W. (1992): Modeling water erosion due to overland flow using physical principles, 2. Rill flow. *Water Resour. Res.*, **28**(1), 245–250.
- 6) Komura, S. (1976): Hydraulics of slope erosion by overland flow. *J. Hydraul. Div., ASCE*, **102**(HY10), 1573–1586.
- 7) Komura, S. (1982): A method for estimating slope erosion by overland flow. *Proc. 37th Annu. Conf. Jpn. Soc. Civ. Eng.*, **2**, Jpn, 483–484 [In Japanese].
- 8) Michael C., Hirschi & Barfield, B. J. (1988): KYERMO—A physically based research erosion model, Part I Model development. *Trans. ASAE*, **31**(3), 804–813.
- 9) Moore, I. D. & Burch, G. J. (1986): Sediment transport

- capacity of sheet and rill flow: Application of unit stream power theory. *Water Resour. Res.*, **22**(8), 1350–1360.
- 10) Mosley, M. P. (1972): An experimental study of rill erosion. M.S. thesis, Colo. State Univ., Fort Collins.
 - 11) Mosley, M. P. (1974): Experimental study of rill erosion. *Trans. ASAE*, **17**(5), 909–913, 916.
 - 12) Nearing, M. A. et al. (1989): A process-based soil erosion model for USDA-Water Erosion Prediction Project Technology. *Trans. ASAE*, **32**(5), 1587–1593.
 - 13) Takagi, A., Tsutsumi, S. & Nakano, M. (1989): Predicting rill erosion and sediment yield. *Trans. JSIDRE*, **141**, 89–98 [In Japanese with English abstract].
 - 14) Takagi, A., Nakao, S. & Tomosho, T. (1993): Predicting sediment discharge from an interrill area by Komura's erosion model. In Proceedings of 48th Chugoku-Shikoku regional conference of JSIDRE, Tokushima, Japan, 78–80 [In Japanese].
 - 15) Yang, C. T. (1973): Incipient motion and sediment transport. *J. Hydraul. Div. ASCE*, **99**(HY10), 1679–1704.